Appl Plant Sci. 2013 Jul 29;1(8):apps.1300034. doi: 10.3732/apps.1300034

A method for preparing spaceflight RNA*later*-fixed *Arabidopsis thaliana* (Brassicaceae) tissue for scanning electron microscopy[1]

Eric R Schultz [2], Karen L Kelley [3], Anna-Lisa Paul [2], Robert J Ferl [2,3,4,5]

Author information Article notes Copyright and License information

PMCID: PMC4103452 PMID: 25202579

Abstract

• *Premise of the study:* In spaceflight experiments, tissues for morphologic study are fixed in 3% glutaraldehyde, while tissues for molecular study are fixed in RNA*later*; thus, an experiment containing both study components requires multiple fixation strategies. The possibility of using RNA*later*-fixed materials for standard SEM-based morphometric investigation was explored to expand the library of tissues available for analysis and maximize usage of samples returned from spaceflight, but these technologies have wide application to any situation where recovery of biological resources is limited.

• *Methods and Results:* RNA*later*-fixed samples were desalinated in distilled water, dehydrated through graded methanol, plunged into liquid ethane, and transferred to cryovials for freeze-substitution. Sample tissues were critical point dried, mounted, sputter-coated, and imaged.

• *Conclusions:* The protocol resulted in acceptable SEM images from RNA*later*-fixed *Arabidopsis thaliana* tissue. The majority of the tissues remained intact, including general morphology and finer details such as root hairs and trichomes.

Keywords: *Arabidopsis thaliana*, RNA*later*, scanning electron microscopy, SEM, spaceflight

---

Experimental flexibility is a luxury often taken for granted in typical laboratory science. Adapting a protocol in response to unfolding information as the experiment proceeds is a key element in discovery and is standard practice. In spaceflight, this luxury is not as accessible; crew time is highly regulated, orbital resources are limited, and protocols are tightly controlled once in place. In addition, the up-mass available to each researcher is limited, which restricts the choices of experimental treatments and orbital fixation options. These constraints often translate into hard choices that limit the scientific return on investment, including sacrificing the number of replicates to enable additional treatment and fixation scenarios. As a consequence, options that allow maximization of the data obtained from a single sample are highly valued.

Biological experiments are typically required to be segregated based on the analyses to be performed upon return from spaceflight. These segregated conditions are usually either molecular or morphological, due to the separate fixatives required for each application (e.g., Stutte et al., 2006). Investigations focused on transcriptome analyses, for instance, would not be likely to commit a portion of their limited up-mass on samples and associated fixation hardware for morphological applications, and would miss the opportunity to use both morphological and molecular perspectives. These limitations are keenly felt in scenarios where the transcriptome analyses reveal spaceflight-specific patterns of gene expression central to morphological patterns of cell growth and development. This scenario was encountered in a recent spaceflight experiment, in which telemetric imaging revealed interesting spaceflight-associated root morphologies (Paul et al., 2012). All material was fixed on orbit in RNA*later* (Ambion, Grand Island, New York, USA) to facilitate transcriptome analyses on returned samples.

Although it is possible to partition an experiment into molecular and morphological components, using samples that correspond directly to those used in molecular applications would be of extreme value. A single fixation protocol better enables the full use of replicates to support a robust power analysis; all plant material allowed by the up-mass constraints can be dedicated to a single application per orbital treatment. Additionally, the plant material apportioned for microscopy can be taken directly from the pool of material whose balance represents a molecular replicate; thus, any morphologic change seen in these plants would directly reflect the effects of the altered gene expressions from those same plants. Terrestrial field studies could also benefit from this single fixative approach for similar reasons.

Despite its use as a molecular fixative, RNA*later* is not commonly used as a morphologic fixative. RNA*later* fixation produces unclear images with high background staining (Cadoret et al., 2013) and reduces immunofluorescent signals (Zaitoun et al., 2010; Paul and Ferl, 2011). This intracellular occlusion eliminates the possibility of clear subcellular localizations. However, the external morphology appears to be preserved in a fresh-like state, which suggests that RNA*later* may be acceptable for use in scanning electron microscopy (SEM). Two cases in the literature report the use of RNA*later* in a morphological investigation. Behrendt et al. (2011) reported that coral covered in crustose coralline

algae was fixed in RNA*later*, postfixed in 2% glutaraldehyde, rinsed in sodium cacodylate, and postfixed again in OsO_4 prior to SEM investigations. Hofer et al. (2012) used SEM in their study on floral organs of *Clermontia* species using RNA*later* as their main fixative with a hexamethyldisilazane drying step. In the current study, both of the above techniques resulted in significant tissue damage in *Arabidopsis*.

An alternative to fixation in SEM sample preparation is freezing. Cryo-SEM does not require prior fixation, but instead preserves tissues in a fresh-like state for imaging (Koroleva et al., 2010; Sarsby et al., 2012; Yu et al., 2013). However, few laboratories have access to such equipment, and the equipment and operation can often be expensive. Therefore, this study investigated the possibility of emulating cryo-SEM on a standard SEM, a "cryo-analog," where tissue would first be returned to a fresh-like state for freezing prior to imaging.

METHODS AND RESULTS

For process development, test samples of 9–12-d-old *A. thaliana* var. *columbia* (Col-0) or Wassilewskija (WS) (The Arabidopsis Information Resource [TAIR], Columbus, Ohio, USA) were harvested into RNA*later* and fixed overnight at ambient room temperature. Fixed plants, along with freshly harvested individuals of the same age, were washed in distilled water with gentle rocking for four 1-h increments. This washing step was designed to desalinate RNA*later*-fixed samples, as the salt crystals were found to damage tissue during subsequent steps (Fig. 1A, B). Desalination also returned the plants to a fresh-like state (Fig. 1C, D) suitable for flash-freezing. Tissues were dissected immediately following the final wash into 5–10-mm lengths to fit on the SEM sample stage ("stub").

Fig. 1.

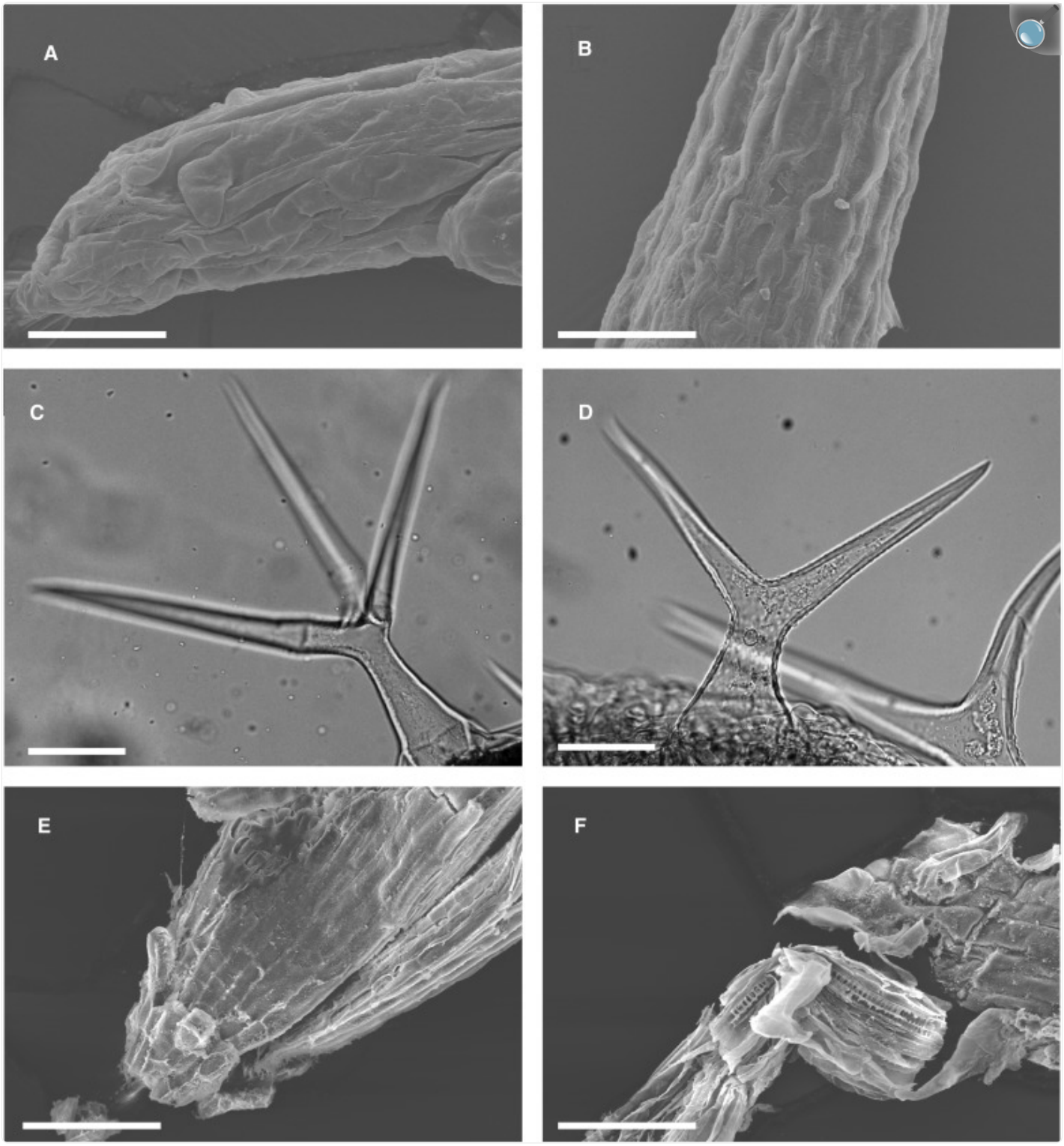

Open in a new tab

Preliminary RNA*later*-fixation investigations. (A, B) *Arabidopsis* root tip (A) and root tissue (B) were

processed through an ethanol dehydration gradient. Tissues were then processed following the protocol in Appendix 1, starting at the critical-point-drying step. No desalination step occurred. 800×, scale bars = 37.5 µm. (C, D) Light microscopy of fresh-harvested (C) and RNA*later*-fixed (D) *Arabidopsis* trichomes displaying similar external morphology. 400×, scale bars = 500 µm. (E, F) *Arabidopsis* root tip (E) and root tissue (F) processed by high-pressure freezing as described in the Methods and Results section. Note fracturing in (F) due to planchette adhesion. 500×, scale bars = 60.0 µm.

The first two protocols tested provided valuable lessons. The first cryo-analog protocol was flash freezing in liquid nitrogen (LN_2). Tissues were severely damaged, primarily due to rapid crystallization of water into ice, physically compromising cellular integrity. The second protocol tested was high-pressure freezing (HPF; Bal-Tec HPM100; Leica Microsystems, Wetzlar, Germany), which resulted in vitrified ice and a greater freezing depth. The noncrystalline structure prevented physical damage, but the roots had a tendency to stick to the planchettes and break (Fig. 1E, F).

The third protocol tested was based on the lessons learned and resulted in minimal tissue damage. The risk of water–ice crystal formation and planchette adhesion was minimized using a variety of methods. Samples were run through a methanol dehydration gradient, starting at 10% and increasing at 10% intervals, for 10 min at each step. An optional wash of 0.1% tannic acid in methanol was used to enhance electron density (Mizuhira et al., 1972; Roholl et al., 1981). *Arabidopsis* tissues were hand-plunged using forceps into LN_2-cooled liquid ethane, which vitrified any remaining water in each sample. These rapid hand-performed plunges provided more control and less damage than automated plunge devices. Samples were immediately transferred to LN_2-cooled individual cryovials, containing either 2% OsO_4 in MeOH or 0.5% glutaraldehyde in 0.1% tannic acid. The headspace in each vial was filled with LN_2 to prevent samples being lost or damaged due to static electric effects. Cryovials were placed into freeze substitution (Leica EM AFS2; Leica Microsystems) to increase the temperature to 10°C over the course of 4–10 d. Cryovial caps were left slightly loose to vent nitrogen gas. Once the temperature reached 10°C, cryovials were removed, opened, and tissues were transferred to tissue baskets (SPI microporous specimen capsules, 120–200 µm pore size; Structure Probe Inc., West Chester, Pennsylvania, USA) while submerged in chilled (4°C) methanol. This transfer took place at ambient room temperature; the chilled methanol submersion is enough to maintain the integrity of the tissues. Individual baskets were labeled using pencil on a small piece of paper approximately 2 mm^2, as external labels were removed during the drying phase. Drying occurred via liquid CO_2 critical point drying (CPD; Bal-Tec CPD 030; Leica Microsystems). Eleven quick-cycled washes replaced most of the loading methanol with CO_2, followed by three 10-min infiltrations. One final exchange was performed and left overnight. Two additional 10-min infiltrations were performed, followed by CPD with controlled venting. Samples were in solution until the end of CPD. Dry samples in baskets were transferred to a desiccant-filled (Drierite; W. A. Hammond Drierite Company, Xenia, Ohio, USA) sealable container until being mounted on stubs using carbon adhesive and returned to a stub rack within a different desiccant-filled sealable container. Mounted samples were sputter-coated for 90 s with a gold-palladium alloy (Desk V HP; Denton Vacuum, Moorestown, New Jersey, USA) and imaged on a scanning electron microscope (Hitachi S-4000; Hitachi, Tokyo, Japan).

Initial observations were focused on roots, resolution of cell files, and retention of root hairs throughout the processing of the tissue (Fig. 2). Later tests observed trichomes and more durable tissues, such as adaxial leaf surfaces and seed coats (Fig. 2A–C). The fresh-frozen tissues, used as protocol development control material, retained finer details, including closed stomata and normal trichome morphology (Fig. 2D, E). RNA*later*-fixed test materials yielded similar images as the fresh-frozen plants, with minimal additional tissue damage (Fig. 2F–K).

Fig. 2.

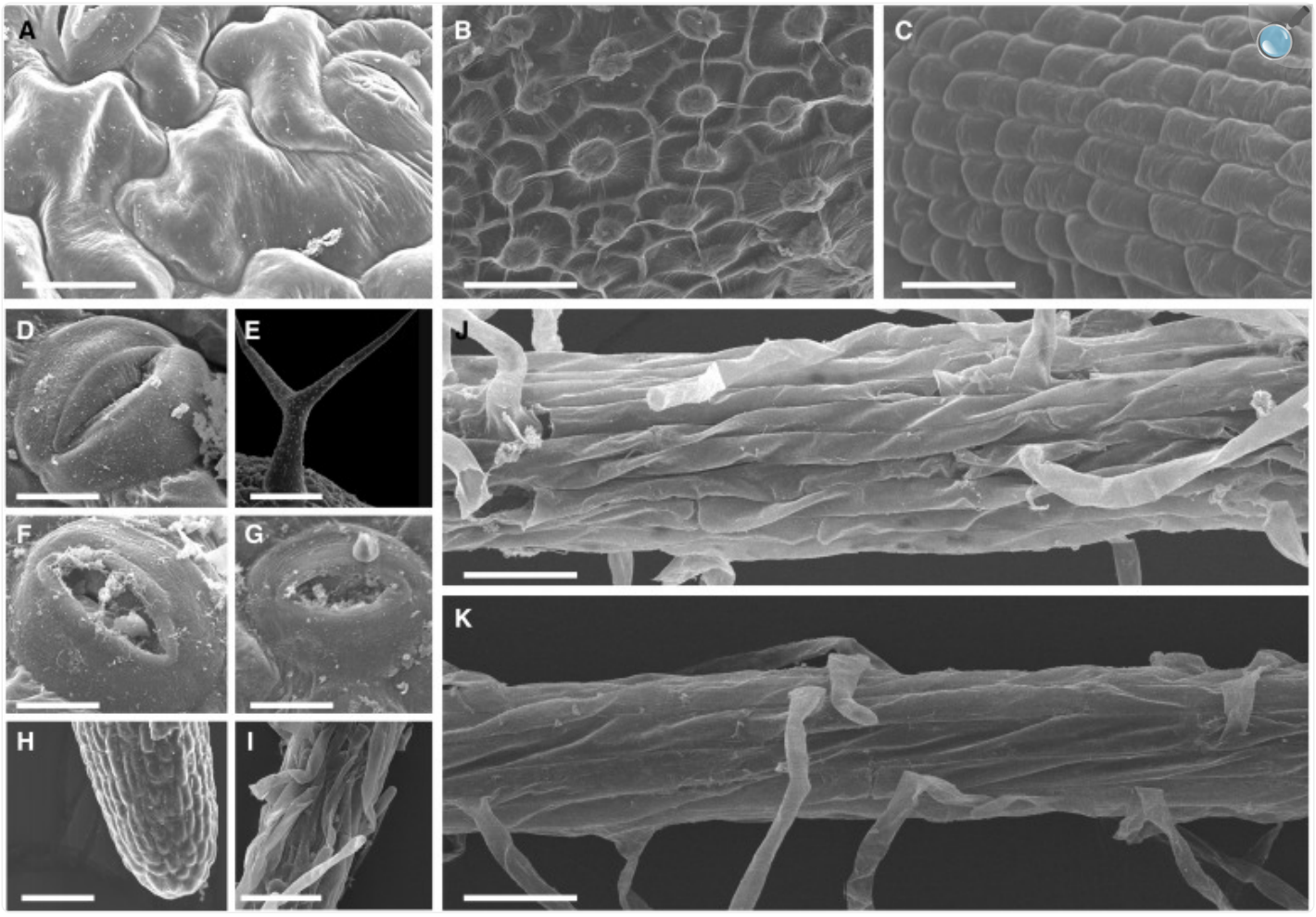

Open in a new tab

SEM images of *Arabidopsis* tissue processed using the protocol described in the Methods and Results section and Appendix 1. (A) Adaxial leaf epidermis (3500×, scale bar = 8.57 μm). (B) Seed coat (900×, scale bar = 33.3 μm). (C) Floral stalk (1300×, scale bar = 23.1 μm). (D) Fresh-harvested stoma (3000×, scale bar = 10.0 μm). (E) Fresh-harvested trichome (447×, scale bar = 67.2 μm). (F) RNA*later*-fixed ground control stoma (3500×, scale bar = 8.57 μm). (G) RNA*later*-fixed spaceflight stoma (3000×, scale bar = 9.99 μm). (H) RNA*later*-fixed spaceflight root tip (500×, scale bar = 30.0 μm). (I) RNA*later*-fixed spaceflight root section (450×, scale bar = 66.7 μm). Obscuring wrinkles are root hairs pressed on root surface. (J) RNA*later*-fixed ground control root section (700×, scale bar = 42.9 μm). (K) RNA*later*-fixed spaceflight root section (700×, scale bar = 42.9 μm).

Spaceflight materials and the corresponding ground controls, both fixed in RNA*later*, were processed using the protocol discussed above and detailed in Appendix 1. Tissues yielded images of acceptable quality, with minimal cell wrinkling and high retention of fine details (Fig. 2J, K). The focus of these samples was root structure, morphology, and root hair retention because of interesting molecular and genetic observations from a recent spaceflight experiment (Paul et al., 2012; Paul et al., unpublished).

Cost of the developed protocol is minimal, while the accessibility is high. Assuming the microscopy core to be used has standard SEM capability, the additional cost of this protocol is merely the cost of consumables. These components are readily available and likely already obtained by the laboratory interested in using this protocol. Another advantage of this protocol is a near retention of tissue morphology at a fresh harvest state. Not only are finer elements of tissues retained (Fig. 2D–I), but other tissues, such as the adaxial leaf epidermis, seed coat, and floral stalk (Fig. 2A–C), produce results comparable to those processed through dedicated morphologic means (e.g., Bhargava et al., 2013). The amount of time needed for this process is slightly longer than other standard SEM processing times, with an additional 4 h for the desalination washes and several days required for freeze substitution. Hand-plunged samples may be processed in batches to increase throughput, being limited to the number of samples able to be held with a pair of forceps without compromising structural integrity. Examples of other SEM protocols may be seen in Liu et al. (2008), Koizumi et al. (2010), Springer et al. (2010), and Yi et al. (2010). As a result of this protocol, samples fixed with RNA*later* retained many fine features including root hairs and trichomes, with a majority of cells inflated and displaying fresh-frozen–like morphology, regardless of whether they were harvested during spaceflight or on the ground.

CONCLUSIONS

The protocol presented here provides distinct advantages for both spaceflight and ground-based experimental applications. *Arabidopsis* plants harvested on the International Space Station by astronauts were successfully retrieved from RNA*later* and processed to produce acceptable quality images without the use of a dedicated morphologic fixative (Fig. 2J, K). Field studies may also benefit from the use of this protocol. As in spaceflight, the amount of materials able to be carried and used during an expedition is limited. With the option of using one stable, safe chemical fixative for all desired studies to be conducted upon return, scientists in the field may be able to collect more data with fewer trips. This protocol may also assist laboratories with libraries of samples in RNA*later* by expanding the available techniques for study.

Alternative imaging techniques outside the scope of this investigation provide alternatives to this protocol. True cryo-SEM would likely be an acceptable alternative (examples may be seen in Koroleva et al., 2010; Sarsby et al., 2012; and Yu et al., 2013), though desalination of specimens prior to tissue processing would still be beneficial. A second option is a cryo-holder, seen in Tang et al. (2012), which may prove to be an acceptable alternative step in this protocol if the SEM being used can handle the LN_2 vapors. A third alternative is scanning ion conductance microscopy (SICM; Marti et al., 1988; Hansma et al., 1989; Ushiki et al., 2012). Due to the high ionic content of RNA*later* and the necessity for

an ionic submersion liquid for SICM, it is possible that this instrument could generate comparable images without any tissue processing. This possibility was not tested due to lack of access to the necessary equipment.

The protocol reported here will likely require optimization for each desired tissue to be tested. *Arabidopsis* is a very fragile tissue, with limited flat surfaces and small organ sizes. Other plants that may be more robust may tolerate a rougher technique, while more fragile tissues (i.e., floral tissues) may need a more gentle approach. Some potential additional steps to enhance tissue integrity include a postfixation step or reversing CPD and sputter-coating. A postfixation step (as seen in Behrendt et al., 2011), which would take place after the desalination, could improve tissue integrity during the cryo-analog plunge, especially if fixatives for electron microscopy, such as Karnovsky's or OsO_4, are used. Sputter-coating prior to CPD (as seen in Yi et al., 2010) may also improve the physical tissue integrity, though both mounting prior to CPD and pulling a vacuum during the coating process may prove difficult.

The use of this protocol provides more morphological opportunities for samples that would have previously been wasted due to improper fixation. It is designed to be a supplement to rather than a replacement of SEM standard practices. Although this process needs to be adapted to each sample being studied, it enhances flexibility in experiments when the main objective is not imaging.

Appendix 1.

Generalized protocol for RNA*later*-fixed sample preparation for SEM investigation.

1. Wash samples in distilled H_2O for four 1-h increments.

2. Dissect samples to fit onto SEM stubs and place into SPI microporous specimen capsules (120–200 μm pore size; Structure Probe Inc., West Chester, Pennsylvania, USA).

3. Dehydrate in graded MeOH (10–100%, 10% intervals) at 10 min per step.

4. Plunge in LN_2-cooled ethane.

5. Immediately transfer to cryovials containing either 2% OsO_4 in MeOH or 0.5% glutaraldehyde in 0.1% tannic acid in acetone.

6. Freeze-substitution (LN_2 at 4°C) for 4–10 d.

7. Perform 11 quick washes (start with MeOH in chamber; cool 10°C for CO_2), followed by three infiltrating washes, leaving the final overnight.

8. Perform two additional infiltrations prior to critical point drying.

9. Critical point dry samples following manufacturer's guidelines and transfer to dessicant-filled box.

10. Clean stubs (if necessary) with acetone sonication.

11. Mount samples on stubs with thick carbon adhesive.

12. Sputter-coat samples for 90 s in gold-palladium alloy.

13. Proceed to SEM imaging.

Chemicals needed: water, RNA*later* (for fixation; Ambion, Grand Island, New York, USA), MeOH (for dehydration), LN_2, ethane, CO_2. Cryovials: OsO_4 and MeOH, or glutaraldehyde, tannic acid, and acetone.

Open in a new tab

LITERATURE CITED

1. Behrendt L., Larkum A. W., Norman A., Qvortrup K., Chen M., Ralph P., Sorensen S. J., et al. 2011. Endolithic chlorophyll *d*-containing phototrophs. The ISME Journal 5: 1072–1076 [DOI] [PMC free article] [PubMed] [Google Scholar]

2. Bhargava A., Ahad A., Wang S., Mansfield S. D., Haughn G. W., Douglas C. J., Ellis B. E. 2013. The interacting MYB75 and KNAT7 transcription factors modulate secondary cell wall deposition both in stems and seed coat in Arabidopsis. Planta 237: 1199–1211 [DOI] [PubMed] [Google Scholar]

3. Cadoret K., Bridle A. R., Leef M. J., Nowak B. F. 2013. Evaluation of fixation methods for demonstration of *Neoparamoeba perurans* infection in Atlantic salmon, *Salmo salar* L., gills. Journal of Fish Diseases 10.1111/jfd.12078. [DOI] [PubMed] [Google Scholar]

4. Hansma P. K., Drake B., Marti O., Gould S. A., Prater C. B. 1989. The scanning ion-conductance microscope. Science 243: 641–643 [DOI] [PubMed] [Google Scholar]

5. Hofer K. A., Ruonala R., Albert V. A. 2012. The double-corolla phenotype in the Hawaiian lobelioid genus *Clermontia* involves ectopic expression of *PISTILLATA* B-function MADS box gene homologs. EvoDevo 3: 26. [DOI] [PMC free article] [PubMed] [Google Scholar]

6. Koizumi A., Yamanaka K., Nishihara K., Kazama Y., Abe T., Kawano S. 2010. Two separate pathways including SlCLV1, SlSTM and SlCUC that control carpel development in a bisexual mutant of *Silene latifolia*. Plant & Cell Physiology 51: 282–293 [DOI] [PubMed] [Google Scholar]

7. Koroleva O. A., Gibson T. M., Cramer R., Stain C. 2010. Glucosinolate-accumulating S-cells in Arabidopsis leaves and flower stalks undergo programmed cell death at early stages of differentiation. The Plant Journal 64: 456–469 [DOI] [PubMed] [Google Scholar]

8. Liu J., Ha D., Xie Z., Wang C., Wang H., Zhang W., Zhang J., et al. 2008. Ectopic expression of soybean *GmKNT1* in *Arabidopsis* results in altered leaf morphology and flower identity. Journal of Genetics and Genomics = Yi Chuan Xue Bao 35: 441–449 [DOI] [PubMed] [Google Scholar]

9. Marti O., Elings V., Haugan M., Bracker C. E., Schneir J., Drake B., Gould S. A., et al. 1988. Scanning probe microscopy of biological samples and other surfaces. Journal of Microscopy 152: 803–809 [DOI] [PubMed] [Google Scholar]

10. Mizuhira V., Futaesak Y., Nishi A. 1972. New fixation method using tannic acid and ultrastructure of microtubules. Journal of Electron Microscopy 21: 233–236 [Google Scholar]

11. Paul A.-L., Ferl R. 2011. Using Green Fluorescent Protein (GFP) reporter genes in RNA*later*™ fixed tissue. Gravitational and Space Biology 25: 40–43 [Google Scholar]

12. Paul A.-L., Amalfitano C. E., Ferl R. J. 2012. Plant growth strategies are remodeled by spaceflight. BMC Plant Biology 12: 232. [DOI] [PMC free article] [PubMed] [Google Scholar]

13. Roholl P. J., Leene W., Kapsenberg M. L., Vos J. G. 1981. The use of tannic acid fixation for the electron microscope visualization of fluorochrome-labelled antibodies attached to cell surface antigens. Journal of

Immunological Methods 42: 285–289 [DOI] [PubMed] [Google Scholar]

14. Sarsby J., Towers M. W., Stain C., Cramer R., Koroleva O. A. 2012. Mass spectrometry imaging of glucosinolates in Arabidopsis flowers and siliques. Phytochemistry 77: 110–118 [DOI] [PubMed] [Google Scholar]

15. Springer D. J., Ren P., Raina R., Dong Y., Behr M. J., McEwen B. F., Bowser S. S., et al. 2010. Extracellular fibrils of pathogenic yeast *Cryptococcus gattii* are important for ecological niche, murine virulence and human neutrophil interactions. PLoS ONE 5: e10978. [DOI] [PMC free article] [PubMed] [Google Scholar]

16. Stutte G. W., Monje O., Hatfield R. D., Paul A. L., Ferl R. J., Simone C. G. 2006. Microgravity effects on leaf morphology, cell structure, carbon metabolism and mRNA expression of dwarf wheat. Planta 224: 1038–1049 [DOI] [PubMed] [Google Scholar]

17. Tang C. Y., Huang R. N., Kuo-Huang L. L., Kuo T. C., Yang Y. Y., Lin C. Y., Jane W. N., et al. 2012. A simple cryo-holder facilitates specimen observation under a conventional scanning electron microscope. Microscopy Research and Technique 75: 103–111 [DOI] [PubMed] [Google Scholar]

18. Ushiki T., Nakajima M., Choi M., Cho S. J., Iwata F. 2012. Scanning ion conductance microscopy for imaging biological samples in liquid: A comparative study with atomic force microscopy and scanning electron microscopy. Micron (Oxford, England) 43: 1390–1398 [DOI] [PubMed] [Google Scholar]

19. Yi B., Zeng F., Lei S., Chen Y., Yao X., Zhu Y., Wen J., et al. 2010. Two duplicate *CYP704B1*-homologous genes *BnMs1* and *BnMs2* are required for pollen exine formation and tapetal development in *Brassica napus*. The Plant Journal 63: 925–938 [DOI] [PubMed] [Google Scholar]

20. Yu Z., Chen H., Tong Y., Wu P. 2013. Analysis of rice root hair morphology using cryo-scanning electron microscopy. Methods in Molecular Biology (Clifton, N.J.) 956: 243–248 [DOI] [PubMed] [Google Scholar]

21. Zaitoun I., Erickson C. S., Schell K., Epstein M. L. 2010. Use of RNAlater in fluorescence-activated cell sorting (FACS) reduces the fluorescence from GFP but not from DsRed. BMC Research Notes 3: 328. [DOI] [PMC free article] [PubMed] [Google Scholar]